heritage

MDPI

Article

On the Thermal Resilience of Venetian Open Spaces

Barbara Gherri [1,*], Daniela Maiullari [2,3], Chiara Finizza [1], Marco Maretto [1] and Emanuele Naboni [1,4]

[1] Department of Engineering and Architecture, Università di Parma, 43125 Parma, Italy; chiara.finizza@unipr.it (C.F.); marco.maretto@unipr.it (M.M.); emanuele.naboni@unipr.it (E.N.)
[2] Department of Urbanism, Faculty of Architecture and the Built Environment, Delft University of Technology, 2628 Delft, The Netherlands; d.maiullari@tudelft.nl
[3] Department of Architectural Theory and Methods, Faculty of Architecture and Civil Engineering, Chalmers University of Technology, 41296 Gothenburg, Sweden
[4] The Royal Danish Academy of Fine Arts, Institute of Architecture and Technology, School of Architecture, Design, and Conservation, 1435 Copenhagen, Denmark
* Correspondence: barbara.gherri@unipr.it; Tel.: +39-0521905956

Abstract: Venice is known for its urban heritage fragility. The city is experiencing an increase in yearly average temperatures affecting outdoor–indoor comfort and average energy expenditure. Owing to existing literature demonstrating how local microclimate depends on urban density, form, and materials, this investigation studies the influence of the changing local climate on Venetian vernacular open spaces, known as *Campi*. Based on the comparison of contemporary weather and the Intergovernmental Panel on Climate Change's (IPCC) future predictions for the 2050 scenario, this investigation highlights how *Campi*'s open spaces and the surrounding buildings, canals, and green public areas contribute to building climate resilience. By employing advanced modelling, the study analyses microclimate and outdoor comfort with respect to users' perception of Physiological Equivalent Temperature (PET). The ENVI-met tool is used to simulate the thermal behaviour of two representative *Campi*: SS. Giovanni e Paolo and S. Polo. Despite significant temperature growths, Venetian urban fabric characteristics seem to play a crucial role in strengthening the climate resilience of open spaces, thus preserving outdoor comfort quality in a warmer future. The analysis shows how the historical matrix of open spaces and buildings cooperate. Thus, this study offers a contribution to how built heritage should be considered in light of climate change.

Keywords: climate change; climate resilience; outdoor comfort; urban form; Venice

Citation: Gherri, B.; Maiullari, D.; Finizza, C.; Maretto, M.; Naboni, E. On the Thermal Resilience of Venetian Open Spaces. *Heritage* **2021**, *4*, 4286–4303. https://doi.org/10.3390/heritage4040236

Academic Editor: Tor Broström

Received: 26 August 2021
Accepted: 8 November 2021
Published: 12 November 2021

1. Introduction

Global warming is likely to reach 1.5 °C in 2030 [1,2]. These phenomena interplay with the Urban Heat Island (UHI) such that urban dwellers experience discomfort due to low-speed wind and thermal radiative exchange [3]. Urban overheating has been documented for more than 400 major cities in the world. According to Santamouris, "numerous studies have shown that global climatic change generating serious heatwave events may act synergistically relative to urban heat islands and further increase the magnitude of urban overheating during extreme climatic events" [4]. Experimental data show that the magnitude of the average temperature increase may exceed 4–5 °C, while at the peak, it may exceed 10 °C [5]. Increased ambient temperatures cause serious impacts on urban environmental quality, local vulnerability, and outdoor comfort conditions such as heat-related mortality and morbidity.

In this context, the city of Venice (IT) experienced a 1.2 °C increase in temperature between 2000 and 2018 related to the 20th-century average [6]. Venice is built on islands and canals, and its close water connection has caused around 3550 floods between 1966 and 2019. The most evident effect of climate change in Venice is the tidal flow: On average, Venice flooded 67 times a year [7,8]. These events have a strong seasonal trend, and they are exacerbated by global warming. In addition to these recurrent phenomena, the number

of hot days in the Venice area (above 27 °C over a 24 h average) went from 0.3 days per year in the 20th century to 9.5 per year in the years since 2000 [6]. Despite this evidence, only a few scientific studies focus on climate change issues that affect the Venice mainland with regards to heatwaves only [9]. Prolonged and intense heat waves affect the city's liveability and energy demand. One of the opportunities for reversing cities' climate change is to develop thermal resilient design measures. These measures can minimize the localized changes of local microclimates. According to Naboni, "A space is thermally resilient if it is able to achieve desirable thermal levels despite the overarching event of climate change . . . The desirable thermal level would be those that are comfortable to people and that is positively allowing the ecosystem to positively evolve...As such universal thermal thresholds cannot be defined universally but should be locally studied" [10].

In this context, urban form considers the configurations of cities that directly affect both outdoor and indoor climates and that have a direct consequence on embodied energy and energy use [11]. Several morphological studies assessed the sustainability of urban form and criteria for urban energy resilience [12]. On the other hand, some studies are investigating the parameterized ideal urban forms resilience [13]. However, no studies are investigating how historical neighbourhoods in dense cities, such as Venice, can respond to climate change issues, especially during heatwaves.

Urban morphology deals primarily with urban form or urban textures, with the shape and dimensions of the built environment, and with the aggregations and configurations of building types. One of the main opportunities for fostering thermal resilience to climate change is predicting the influence of urban form on the local microclimate. In the field of the built environment, several frameworks have been developed for assessing urban energy resilience [14]. Previous studies have shown the increasing importance of taking microclimatic conditions into account when analysing the outdoor spaces' liveability and building energy performance [15,16]. Urban form [17], building density [18] and urban compactness [19], construction materials, and anthropogenic heat are proven to drastically influence local thermal distribution and wind patterns. Recent European projects have taken the innovative approach of correlating high-resolution climate change scenarios with building simulation tools to investigate the potential impacts of climate change on Europe's cultural heritage assets, particularly focusing on historic buildings and their indoor environment [20].

What is still underestimated is how historic, dense cities with consolidated urban configuration/structure can respond to climate change impacts.

Given that the typical trait of Venice is the irregularity of the urban fabric, the focus of this research is to assess to what extent typical irregular patterns determine Urban Heat Island phenomenon and how open areas such as Venetian *Campi* are thermally resilient to heatwaves in the current and 2050 projected scenarios. This paper is based on software-based microclimatic analysis and the Physiological Equivalent Temperature (PET) [21] index evaluation of two specific urban archetypes of *Campi* (240 m × 240 m) in contemporary and 2050 climatic scenarios. The analysis focuses on the role of typical Venetian open space in strengthening the thermal resilience of built heritage relative to climate change and in preserving outdoor comfort in a warmer future.

2. Background

2.1. Urban Form and Urban Resilience in Historical Cities

Urban resilience to heatwaves has been debated over the past decades, originating from its origins in ecology, including modern city and urban planning. Most of the studies on urban resilience are focused on the following: (i) densely populated cities that have suffered severe damages from climate change (i.e., Cape Town and New Orleans) [22]; (ii) UHI mitigation and buildings' materials [23]; (iii) urban heat resilience thanks to the presence of large urban parks [24]; and (iv) urban texture on building energy consumption [25]. A resilience thinking approach in the historical city is mainly focused on the preservation of cultural heritage; nevertheless, few studies are available for Italian cities

such as Bologna, Milan, Florence, and Rome [26], with only a few references to historical urban fabrics and their resilience potential in facing local warming. Recent studies have explored the interrelations between urban form and annual energy performance, expanding urban environmental analysis from energy performance to new environmental quality-based considerations [27,28]. Nonetheless, historical cities' resilience must be investigated thoroughly, as the link among microclimatic issues with urban form, surface-to-volume ratios, use patterns, and building materials needs to be studied.

Urban fabric's effects on building energy consumption and daylight availability [29] are significant: The pattern of streets, building heights, open spaces, green masses, water bodies, and soil sealing degree influence environmental quality both outside and inside the buildings. As Givoni states: "The outdoor temperature, wind speed and solar radiation to which an individual building is exposed is not the regional synoptic climate, but the local microclimate as modified by the "structure" of the city, mainly of the neighbourhoods where the building is located" [30].

The European Commission in the last decades has renewed its interest in the compact city as a sustainable and resilient urban form, indicating the dense and compact city as the solution to pursue urban efficiency and urban quality: "We must conceive of our towns and cities in terms of the dense, compact urban form requiring as few resources as possible for their maintenance and allowing their inhabitants to have access to various urban functions and services in the immediate vicinity, as well as to leisure areas and preserved natural areas . . . Our towns and cities must be coherent and compact if urban areas are to be made easier, more accessible and livelier for all their inhabitants..." [31].

However, highly dense urban environments increase urban overheating due to heat-trapping mechanisms. Urban compactness significantly modifies energy balance in cities, influencing the intensity of the UHI effect, the solar radiation availability on buildings' façade, and wind and breezes distribution. In the Mediterranean climate, the relationship between compactness, solar access in urban textures, and energy demand has been deeply studied, highlighting the possibility of enhancing thermal comfort through the optimization of urban form. According to the literature, although increasing urban compactness implies a decrease in solar energy availability within the urban texture during the daytime, at night it substantially contributes to increasing UHI intensity in urban areas [17,32]. Consequently, urban overheating can potentially reduce human comfort in outdoor and indoor spaces and harm space liveability and human health. The case of Venice is, therefore, peculiar because of the presence of large open areas such as *Campi* surrounded by highly compact fabrics and a large presence of canals.

2.2. Urban Form in Venice Campi

The urban form of Venice derives from historical sedimentations dated back several centuries [33]. Three urban configurations (Figure 1) can be found in Venice [34]: (i) the quadrangular *Campo* (Byzantine period), located in the heart of self-sufficient islands; (ii) the "bone structure" (Gothic age), with primary water and land routes, on parallel axes spaced from secondary structures such as calli, communal courtyards, and large individual houses; and iii) the *Fondamenta* type (the comb structure) (modern age), a street parallel to a canal. They serve as a base/foundation, with houses aligned to foundations or transversal to courtyards and streets.

In all three urban patterns, *Campi* represent the cores of Venice's urban life. *Campi* can vary in size: from small *Campielli* to larger squares. According to Crowhurst Lennard's essay [35], "The *Campo* is an open, irregularly shaped paved space surrounded by buildings. These buildings, which vary in height up to five stories, and in importance and purpose, often contain small businesses and services on the ground floor and private dwellings above".

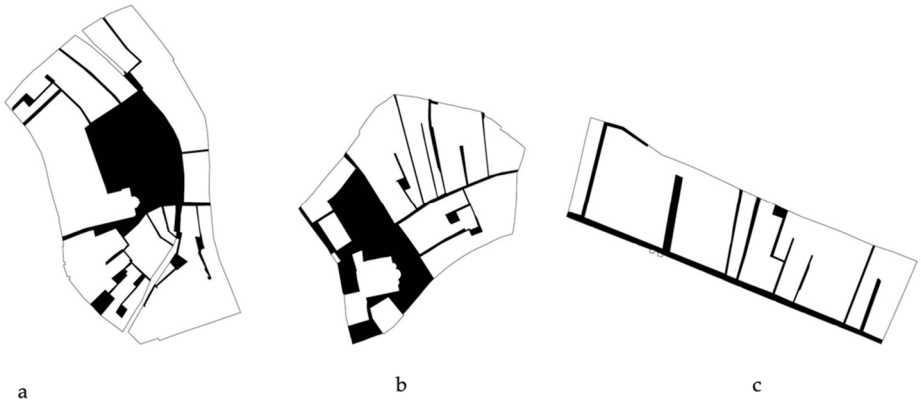

Figure 1. Venice's urban configurations: quadrangular (**a**); bone (**b**); *Fondamenta*—comb (**c**).

In this study, the Venetian vernacular open areas of *Campi* are used as samples to investigate urban fabric typical configurations and resilience to heat waves due to climate change. Two different Venetian *Campi* are selected as in Figure 2.

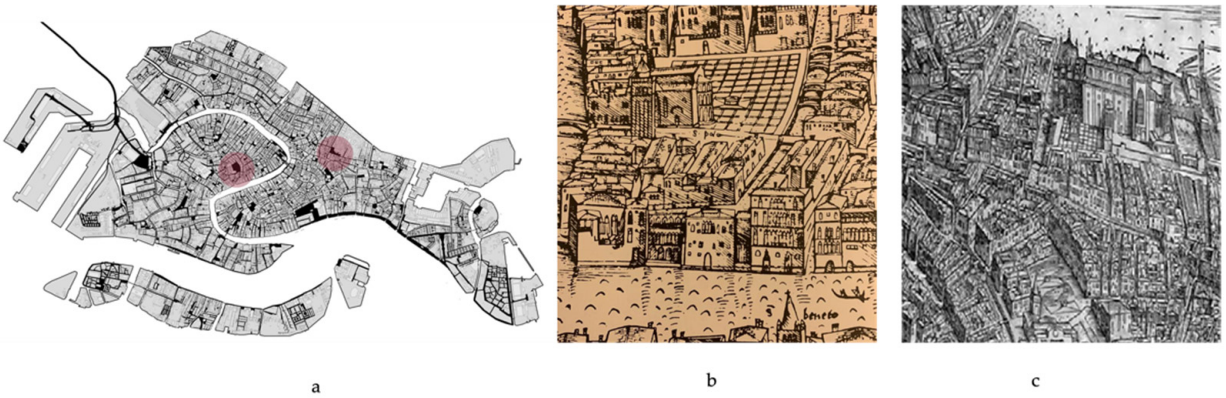

Figure 2. Venice and two selected *Campi* (**a**); San Polo in de' Barbari illustration (1500) (**b**); SS. Giovanni e Paolo in de' Barbari (1500) illustration (**c**).

The first, *Campo* San Polo, is one of the typical "parish islands" built in Venice in the 10th–11th centuries, and it is the largest in Venice. It connects the *Canale di Cannaregio* and San Marco districts. *Campo* S. Polo developed nearby one of the main Venetian waterways, just behind the *Palizzada* del Canal Grande (Figure 3b,c). The main communication route is the canal, San Polo Rio, as streets act similarly as secondary paths. Buildings in this *Campo* feature a double internal courtyard that forms homogeneous fronts, known as *Palizzada* di S. Polo.

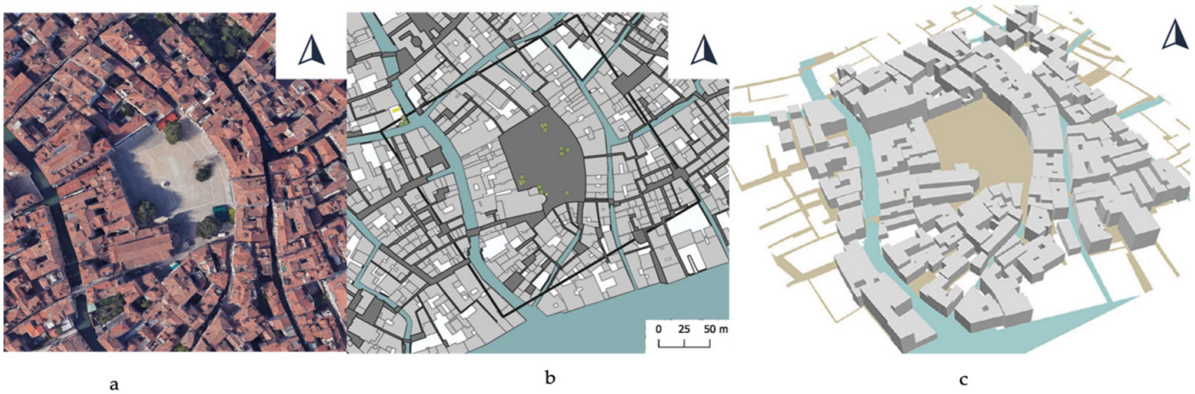

Figure 3. Aerial view of *Campo* San Polo (**a**) and morphological map (**b**); axonometric view of the selected 240 m × 240 m area (**c**).

Buildings are quite irregular in their heights (10–20 m), with a maximum height of 26,6 m and a mean height of 12.62 m (Figure 3c), as they were built in different periods and following canals' obstruction. The open space of the *Campo* is also shaped by the Church of S. Paolo Apostolo. According to Spacematrix indexes [36], San Polo has a Floor Space Index (FSI) of 2,29, Ground Space Index (GSI) of 0.57, and Open Space Ratio (OSR) of 0.18.

The second key-selected area is *Campo* SS. Giovanni e Paolo (Figure 4), located between the Cannaregio and Castello neighbourhoods. It is located at the intersection between the *Canale della Misericordia* and an east-west axis, built behind *Rio de S. Giovanni Laterano*. This *Campo* developed along with one of the most important fringe belts of the Gothic city (dated back to the XIV-XV century) when a great urban space availability resulted in the construction of monastic and hospital buildings. Great Scola di San Marco is the most relevant building in the *Campo*. Along with *Canale della Misericordia* and numerous Gothic buildings with limited heights, they form a homogeneous building front. On the other side, the *Campo* is completely open along the Misericordia Canal. The latter is obstructed by the monastery walls as, near Rio de Santa Marina, a more regular and less dense fabric can be found. The focus of the square is Santi Giovanni e Paolo Church [37], for which its maximum height is 50.70 m (Figure 4c) with a Floor Space Index (FSI) of 2.73, Ground Space Index (GSI) of 0.67, and Open Space Ratio (OSR) of 0.12.

Figure 4. Aerial view of *Campo* SS. Giovanni e Paolo (**a**) and morphological map (**b**); axonometric view of the selected 240 m × 240 m area (**c**).

These two *Campi* were selected due to their different orientation, building density, spatial configurations, and relation to the waterways. They represent an excerpt of the typical Venetian open spaces with limited extension if compared to other vernacular Italian squares, and the neighbourhood's social activities take place in these locations.

3. Materials and Methods

The proposed research aims to investigate the thermal resilience of Venice *Campi* today and in future climates.

In order to fulfil the aim, present and future weather scenarios (2050) are analyzed, firstly via a qualitative solar shading analysis and then via ENVI-met. The paper responds to three main objectives: (i) assess today's thermal stress of selected *Campi* (San Polo e SS. Giovanni e Paolo); (ii) assess the climate change thermal stresses in the projected 2050 climatic scenario; and (iii) discuss resilience potentialities and constraints.

To analyse the thermal performance of the two *Campi*, this study employs a climate modelling approach. Microclimate simulations are widely used to compute air and surface temperatures, turbulence, radiation fluxes, humidity, and evaporation fluxes.

ENVI-met 4.4, a three-dimensional prognostic software, has been used for this purpose. Previous studies have employed ENVI-met to simulate the interaction between air, plants, and surfaces within an urban environment [38,39]. This tool supports the analysis of the impact of the UHI phenomenon on the outdoor thermal comforts of different form patterns [40,41] and the evaluation of heat mitigation strategies' efficacy [42,43]. Validation

studies have also confirmed its good level of accuracy in modelling microclimate processes in urban conditions [44] and the high sensitivity of the tool to morphological characteristics of the built environment [45].

3.1. Climate Datasets and Microclimatic Simulations

The modelling of the two climate scenarios in 2020 and 2050 is based on two climate datasets. The standard EPW file of Venice [46] is used as a contemporary climatic reference. The nineteenth of August is selected as simulation day. It is a typical summer day with clear skies, according to the STAT file analysis.

The Meteonorm Climate Generator [47] is then employed to project the 2050 climate scenario based on the Intergovernmental Panel on Climate Change (IPCC) scenario A1B. The selected A1B scenario is characterised by a balanced development of energy technologies on all energy sources. A1B scenario considers a predictive future scenario in between a fossil fuel-intensive future development (A1FI) and a predominantly non-fossil fuel future (A1T). 2050 projected EPW file is developed according to the A1B scenario, as described in the Special Report on Emissions Scenarios (SRES) [48].

With the combination of Meteonorm's current database 1961–90, the interpolation algorithms and the stochastic generation typical years can be calculated for any site, for different scenarios, and any period between 2010 and 2200. Meteonorm can, therefore, be used as a relatively simple method for enhancing spatial and temporal resolutions instead of using downscaling methods based on regional climate models.

The simulation day in the current data marks an average temperature across the 24 h of 23.7 °C, whereas the 2050 forecast, generated by Metenorm Software by historical time series of irradiation and temperatures, marks a significant difference of 30.5 °C (Figure 5a,b). The variation calculated by Meteonorm assumes that the amplitude of the temperature variation during daytime is approximately proportional to the amplitude of the daily global radiation profile. Therefore, the temperature profiles are calculated by transforming the radiation profile for the current and the projected scenarios. The average wind rises from 206 degrees.

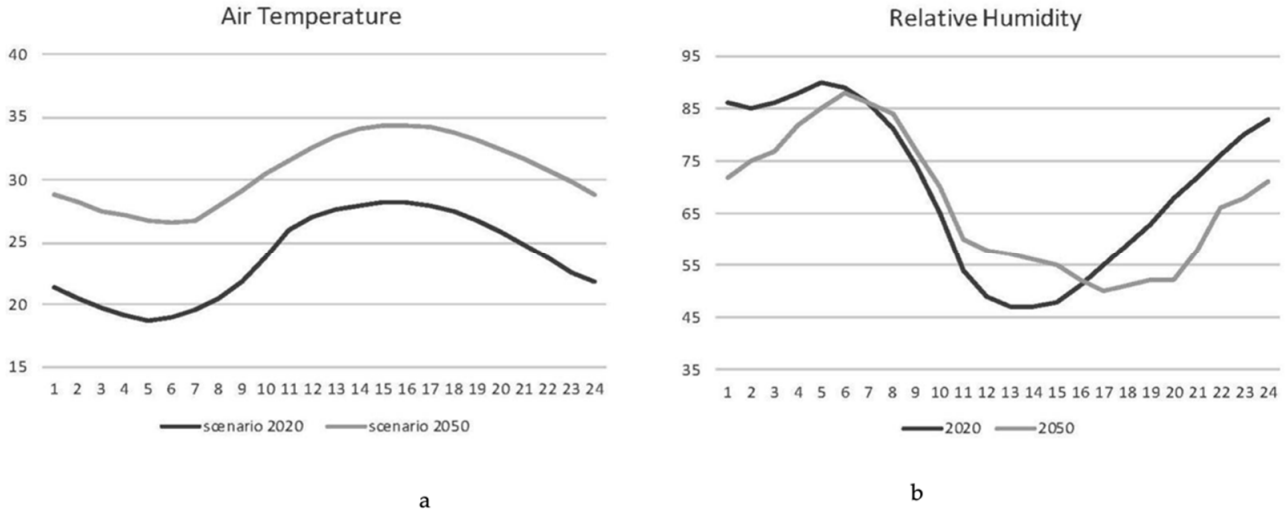

Figure 5. Air temperature profiles in 2020 and 2050 scenario (**a**); relative humidity profile in 2020 and 2050 scenario (**b**) according to A1B scenario, made with Meteonorm.

Shading analyses were also conducted to characterize *Campi*'s thermal performance. Online-tool Shadowmap [49] is used to perform the shadow's path for the 19th August at h. 10 am, at h. 1 pm, and h. 4 pm for both *Campi.*

To perform an ENVI-met simulation, three groups of inputs are required: (i) geometry and material information to build a digital spatial model (Area Input File); (ii) characteristics

of the selected materials to define a material database (Database); and (iii) simulation settings and meteorological input data (Configuration File).

In the Area Input Files, two domains are shaped by using a grid cell unit of 2.0 m × 2.0 m × 3.0 m. Here, the 3D models are built based on the data collected by survey and on spatial data retrieved by the open dataset *Atlante della Laguna* [50]. For the Database, materials and thermophysical properties have been modelled by mostly using the ENVI-met database, since it provides a large variety of materials for buildings, surfaces, and vegetation. In the case of specific materials, such as *Trachite Euganea*, the standard pavement value has been modified according to the literature source [51]. Thus, the material default Database was enriched by including the material thermal properties of the *Trachite Euganea* (a locally quarried stone) for street pavements, exposed brick wall and plastered brick wall for building envelopes, and, finally, shallow water for the canals (1.0 m deep). Tables 1–3 summarises the material information used to run the simulations for the Venice case studies. It is worth noting that the material's properties have been deliberately simplified and kept invariant in the simulation.

Table 1. Venice material profiles used for the microclimatic simulation.

Building Materials	Plaster	Masonry—Heavyweight	Brick-Burned
Absorption (-)	0.50	0.65	0.60
Transmission (-)	0.00	0.00	0.00
Reflection (-)	0.50	0.35	0.40
Emissivity (-)	0.90	0.90	0.90
Specific Heat (J/kg·K)	850	840	650
Thermal Conductivity (W/m·K)	0.60	0.90	0.44
Density (kg/m^3)	1500	1850	1500

Table 2. Venice urban finishing material profiles used for the microclimatic simulation.

Urban Finishing Materials	Trachite Euganea	Canal Water
Roughness (-)	0.01	0.01
Albedo (-)	0.5	0.04
Emissivity (-)	0.9	0.96

Table 3. Venice urban profiles used for the microclimatic simulation.

Building Profiles	Brick-Burned	Plaster	Masonry Heavyweight	Plaster
Exposed Brick Wall	10 cm	0	25 cm	2 cm
Plastered Brick Wall	0	2 cm	40 cm	2 cm
Urban Profiles	Trachite Euganea	Sand	Sandy Loam	
Pavement	6 cm	20 cm	200 cm	
	Water	Loamy soil	Sand	
Canal	100 cm	50 cm	50 cm	

Configuration files are created to simulate the average hot day and the projected same day in 2050. The employed simple forcing method made use of the climate boundary conditions described before. Finally, the four simulations are performed, and the results are studied for a selected number of hours.

3.2. Physiological Equivalent Temperature Index Microclimatic Studies

In the next phase, the two areas' thermal comfort was assessed for the current and projected scenario. ENVI-met results are processed in the sub-module BIO-met 2.0 to

calculate the Physiological Equivalent Temperature (PET) comfort index. This index is based on a prognostic model of the human energy balance that computes the skin temperature and the body core temperature. PET is the universal index used to bio-meteorologically assess the thermal environment, and it shows how changes in the thermal environment can affect human thermal comfort [52].

The assessment relies on obtained microclimatic values of Means Radiant Temperature (MRT), Potential Air Temperature (Pot), Wind Speed (WS), and Relative Humidity (RH) and the target person characteristics. For this study, the target person is 35 years old and 1.75m tall, characterized by a metabolism of 80 W (light activity) in addition to basic metabolism, and by 0.9 clo of heat resistance because of clothing.

In the last phase, the PET values, calculated for the two scenarios, are mapped in the two areas.

Finally, the predominant form and microclimate components that affect the thermal performance of the *Campi* are identified by using a detailed comparative analysis of thermal comfort variations.

4. Results

The comparison is concerned with the thermal comfort patterns for selected hours of the day, with special regard to h. 4 pm, when the worst thermal condition occurs, at the pedestrian level (1.5 m) for 2020 and 2050.

4.1. Campo San Polo Results

4.1.1. Shading Performance

The shading performance of *Campo* San Polo is assessed (Figure 6) at h.10 am, h.1 pm, and h.4 pm. The shadows' path is valuable in providing a global understanding of the solar trajectory inside of the *Campo*. In San Polo, the shaded areas extend for about one-third of the paved open *Campo*. In San Polo, the central part of the *Campo* remains globally unshaded in the three selected hours mainly because of the larger open area and the distance between buildings' façades. The almost total absence of greenery and other obstacles ensures great solar incomes both on vertical and horizontal surfaces.

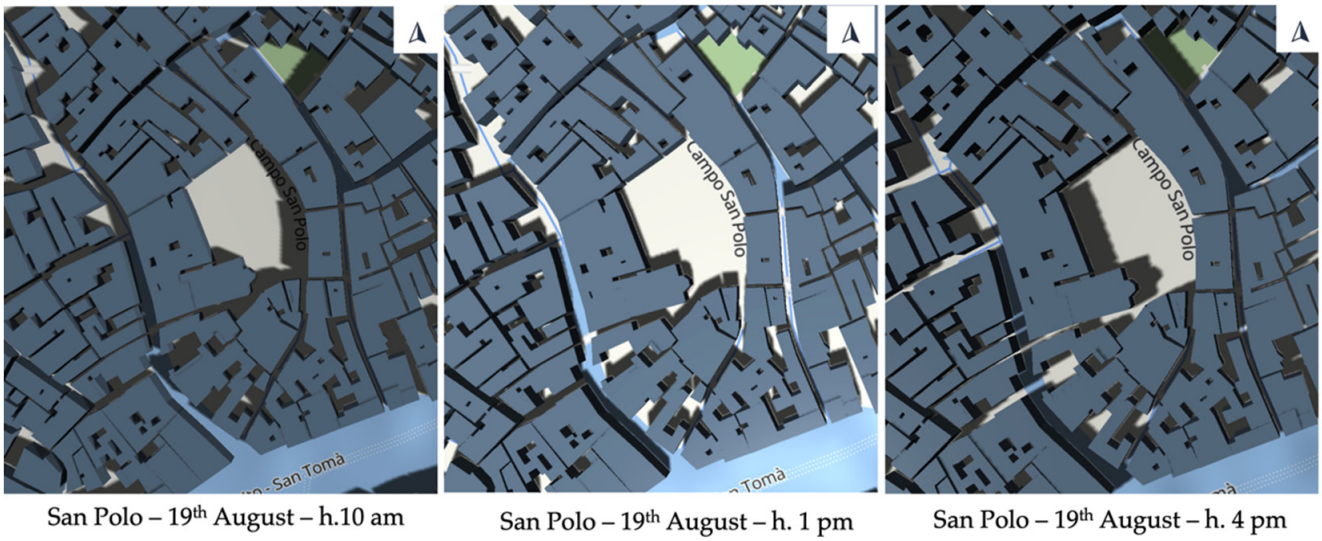

Figure 6. Shadow map visualizes light and shadow on 19 August, considering buildings and terrain, for San Polo.

4.1.2. Thermal Stress Values

In scenario 2020, PET temperatures (Figure 7a) have a homogeneous distribution, moving from a prevalent temperature of 38–41 °C at h.10 am to 41–45 °C at h.4 pm.

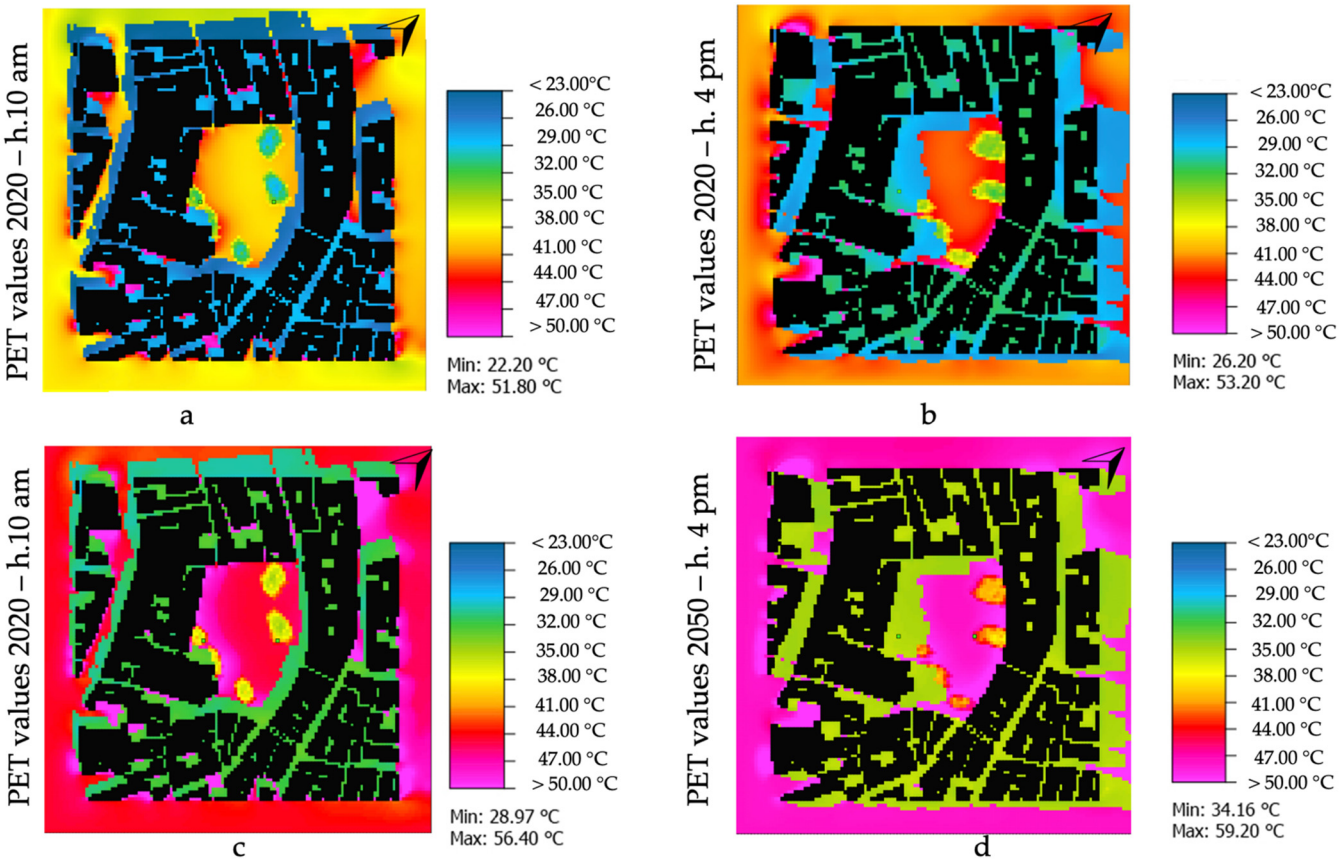

Figure 7. Thermal stress maps for *Campo* San Polo in 2020 in the morning and afternoon (**a**,**b**) and in the projected 2050. scenario (**c**,**d**).

During the three hours, despite the diurnal increase in PET values, vegetation and shadow decrease thermal discomfort in a range of 12–18 °C. In scenario 2050 (Figure 7c,d), PET values maintained the same pattern distribution observed in scenario 2020. Perceived temperatures reach 50 °C already at h.10 am (Figure 7c), while ΔPET is around 3 °C.

Potential Air Temperature (PoT) (Figure 8c) and Wind speed (Figure 8e), calculated at h. 4 pm (hottest hour), are homogeneous due to the similar buildings' height. In 2050, PET (Figure 8f) values slightly increased compared to 2020 conditions (Figure 8a) due to Mean Radiant Temperature (MRT) (Figure 8b) and lower Relative Humidity (RH) (Figure 8d). However, shadow and vegetation's impact tend to increase, mitigating thermal distress in a range of 21–24 °C. Nonetheless, *Campo* San Polo seems to assure extreme heat stress since PET over 41 °C means extreme hot conditions for European cities.

In the compact urban fabric around *Campo* San Polo, the PET difference (Figure 9) is generally lower than 5 °C. This behaviour suggests that high shadow density contributes to mitigating urban heat also in future warmer conditions.

However, in the open space of San Polo, the main variation between the two scenarios is determined by the heat released through convection from the building and pavement surfaces. Higher MRT in the 2050 scenario drastically reduces the beneficial effect of shadow in the open space (Figure 10). These areas, thus, report the highest PET difference of 7 to 6.5 °C (Figure 9), while the areas exposed to sun radiation stay around 6 °C.

4.2. Campo SS. Giovanni e Paolo Results

4.2.1. Shading Performance

A shadow path analysis in SS. Giovanni e Paolo shows that the most effective shadows are cast by the buildings along the canal and by those alongside the church, assuring a larger shaded area in the southern part of the *Campo* (Figure 11). The presence of the church

geometrically divides the *Campo* into two portions. The first portion, the churchyard of the church, remains unshed during the hottest hours; the southern part of the *Campo* benefits only half of its depth from the shadows cast by the buildings' front.

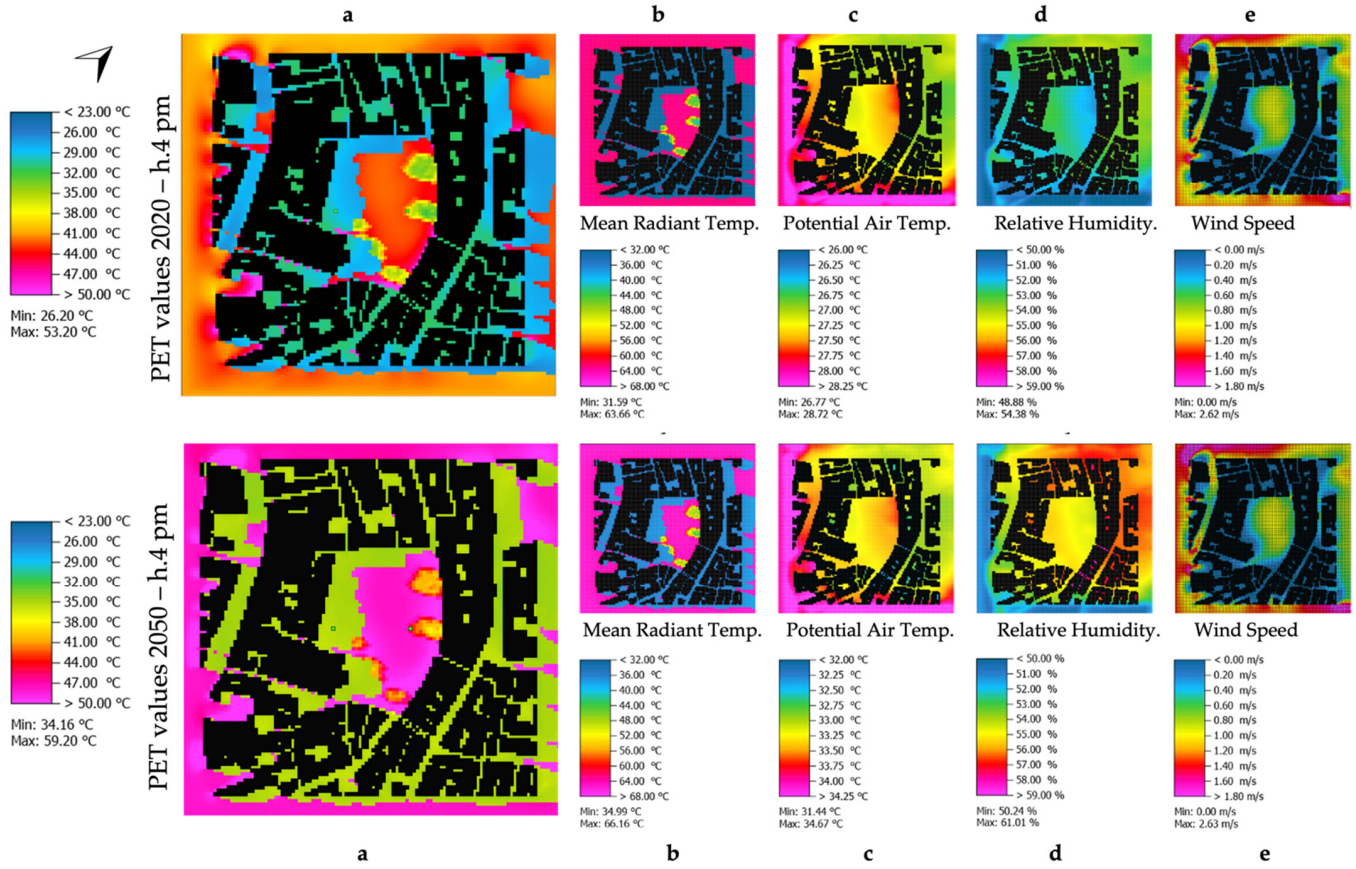

Figure 8. (**a**) Thermal stress maps for *Campo* San Polo in 2020 at h.4 pm (**top**) and projected 2050 scenario (**bottom**) predicted by considering (**b**) MRT, (**c**) PoT, (**d**) RH, and (**e**) Wind speed.

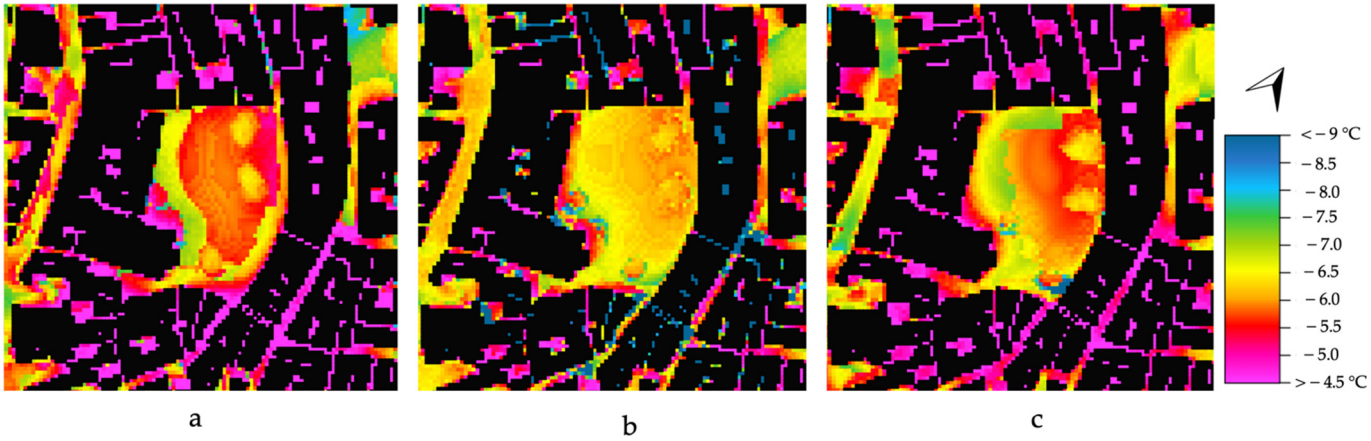

Figure 9. Computed PET difference in *Campo* San Polo in 2020–2050 at h.10 (**a**), h.13 (**b**), and h. 16 (**c**).

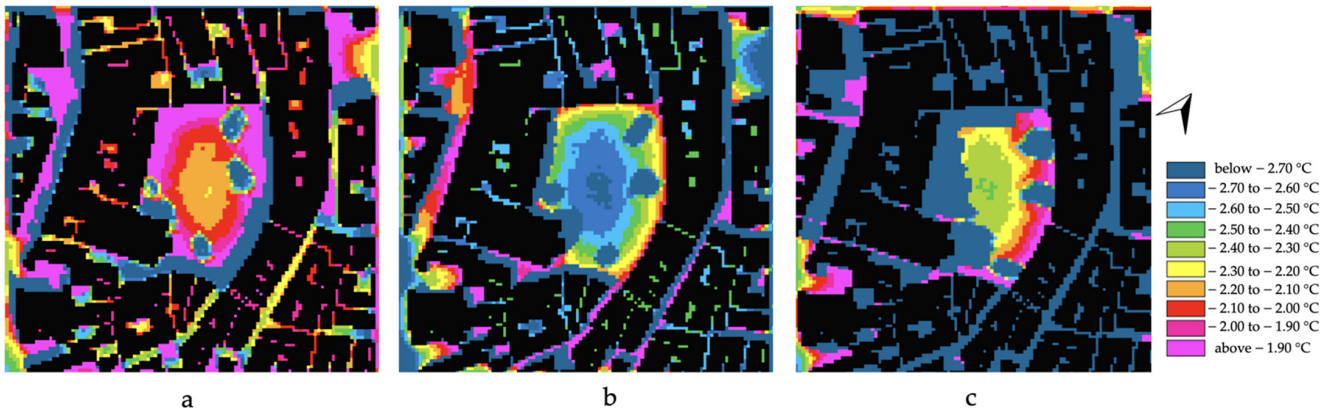

Figure 10. Computed MRT difference in *Campo* San Polo in 2020-2050 at h.10 am (**a**), h.1 pm (**b**), and h. 4 pm (**c**).

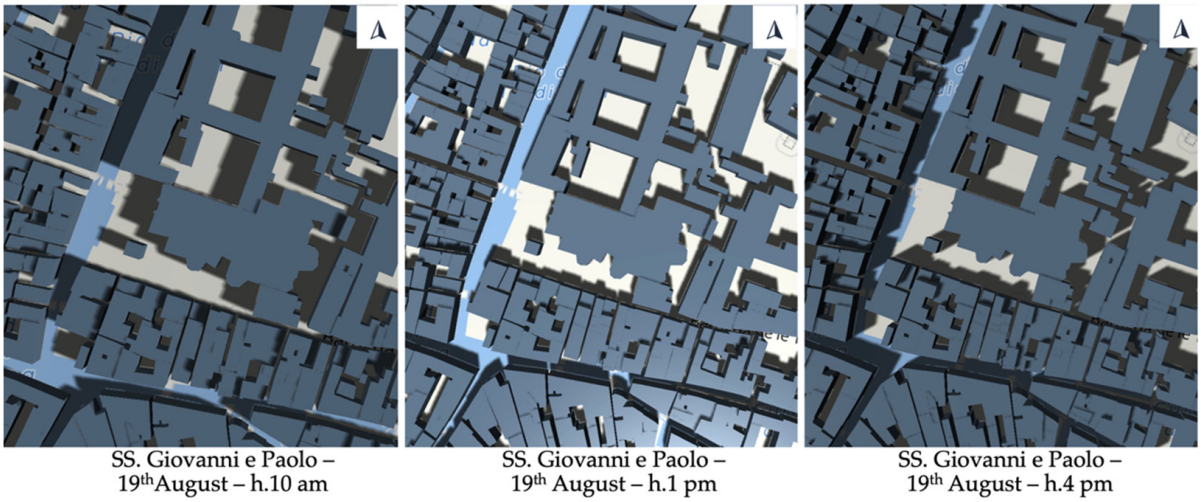

Figure 11. Shadow map visualizes light and shadow on 19 August, considering buildings and terrain, for SS. Giovanni e Paolo..

4.2.2. Thermal Stress Values

Compared to San Polo, *Campo* SS. Giovanni e Paolo shows a more heterogeneous PET value distribution (Figure 12). Scenario 2020 (Figure 12a,b) shows that perceived temperatures tend to be lower in the northwest part of the square and gradually increases towards the southeast side. In the latter, temperatures reach 50 °C in the early morning (Figure 12a) and persist until h. 4 pm (Figure 12b).

Due to vegetation's scarce presence, only building shadow contributes to increasing the comfort level by lowering the perceived temperature. The variations between max PET temperature and minimum temperature in shadow areas are equivalent to around 27 °C at h.10 am (Figure 12a) and 32 °C at h.4 pm (Figure 12b).

Similarly, in scenario 2050, a variation of comfort level was found between the northwest and southeast parts of the *Campo* (Figure 12c,d).

PET temperatures reached a maximum of 60 °C at h.4 pm (Figure 13b), while shadow patterns maintained their beneficial role in reducing thermal stress. A more detailed observation of the microclimate factors affecting PET values in the hottest hours (h.4 pm) shows that shadow patterns play a crucial role. The canal canyon allows wind flow infiltration at a relatively high velocity of 1.8m/s (Figure 13e).

As in San Polo, the same pattern in PET distribution (Figure 14) can be observed in *Campo* SS. Giovanni e Paolo. Here, the variation in the shadowed area can reach 8.5 °C in the early afternoon, while exposed areas retain a variation of 6.5 °C (Figure 14).

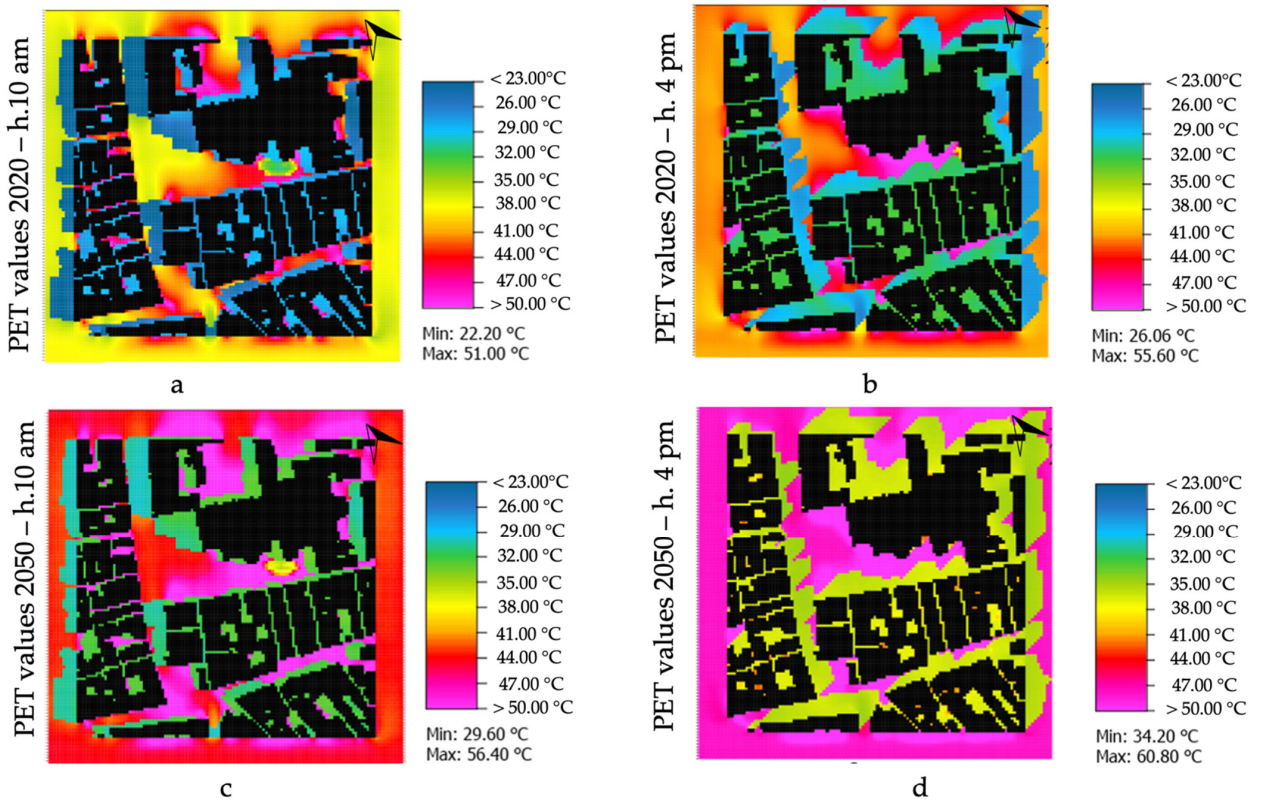

Figure 12. Thermal stress maps for *Campo* Santi Giovanni e Paolo in 2020 in the morning and afternoon (**a**,**b**) and in the projected 2050 scenario (**c**,**d**).

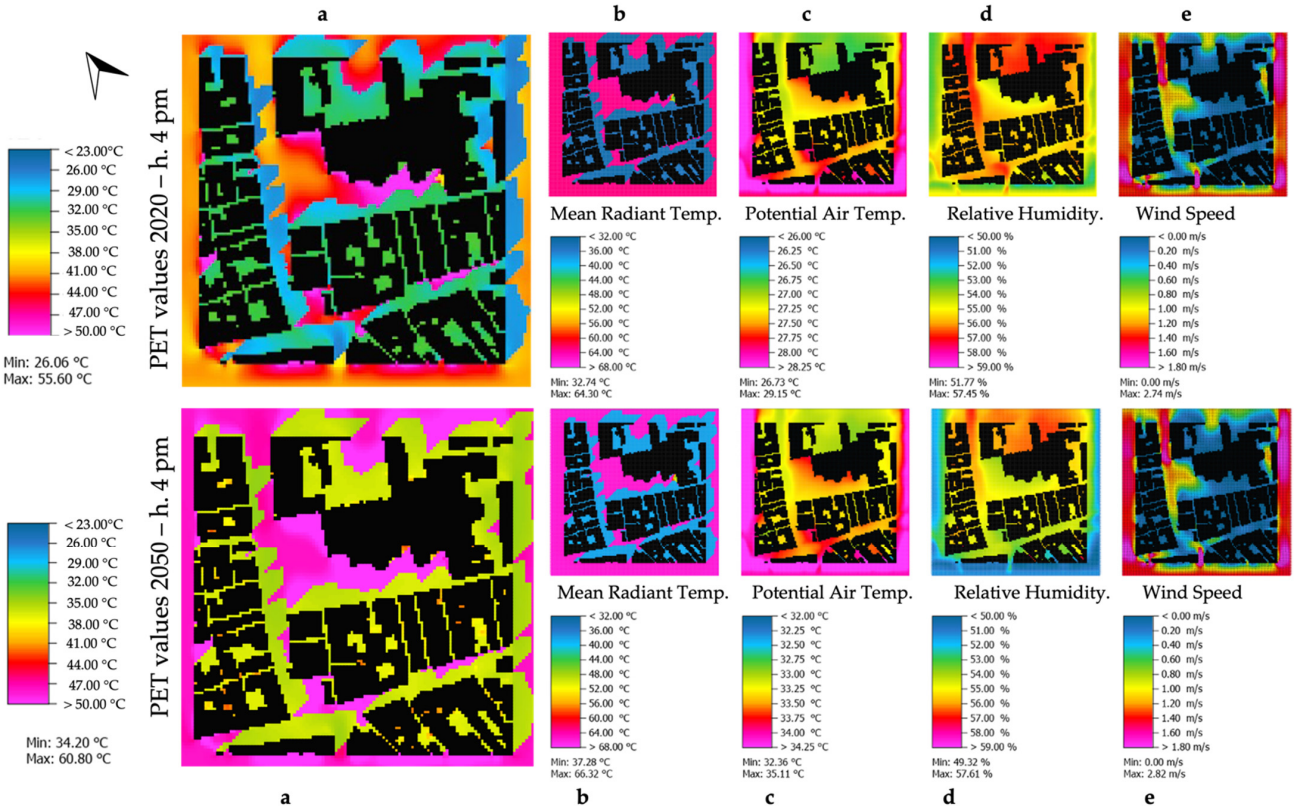

Figure 13. (**a**) Thermal stress maps for Campo SS. Giovanni e Paolo in 2020 at h. 4 pm (**top**) and 2 projected 2050 scenario (**bottom**) predicted by considering (**b**) MRT, (**c**) PoT, (**d**) RH, and (**e**) Wind speed.

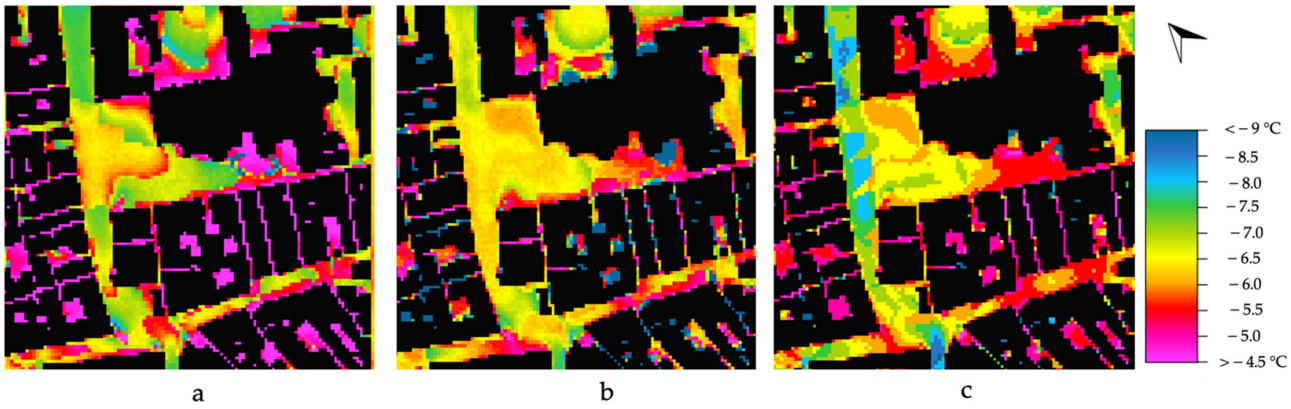

Figure 14. Computed PET difference in *Campo* SS. Giovanni e Paolo in 2020–2050 at h.10 am (**a**), h.1 pm(**b**), and h. 4 pm (**c**).

As in San Polo, higher MRT values in the 2050 scenarios reduced the effect of shadows in the open space (Figure 15). Geometrical and thermal performances for both *Campi* in 2020 and 2050 are compared in Table 4 and in Figure 16.

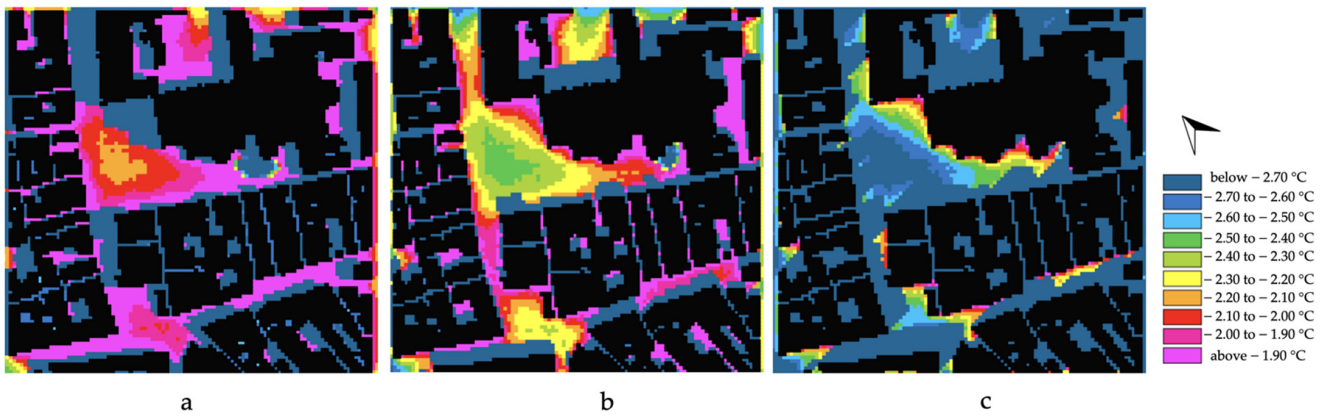

Figure 15. Computed MRT difference in *Campo* SS. Giovanni e Paolo in 2020–2050 at h.10 am (**a**), h.1 pm (**b**), and h.4 pm. (**c**).

Table 4. Geometrical and overall thermal performances for *Campi* in 2020 and 2050.

Data	***Campo* San Polo**	***Campo* SS. Giovanni e Paolo**
Orientation	E-W	N-S
Open paved area (m^2)	5728	3510
Average Buildings Height (m)	0.50	0.35
Maximum Buildings Height (m)	26.6	50.7
Mean Buildings Height (m)	11.55	12.53
Canal orientation	parallel to the *Campo*	parallel to the *Campo*
Canal influence	2 canals-not facing the *Campo*	1 canal-facing the *Campo*
Green Mass	4 trees	1 tree
Green Mass average diameter (m)	16	10
Shaded open area (including the canal) % at h.10 am, h.1 pm, and h. 16 pm	33%; 16%; 30%	23%; 21%; 42%
Δ MRT (2020–2050) at h.10 am, h.1 pm, and h. 4 pm	5 °C (h.10 am); 6 °C (h.1 pm); 6.5 °C (h.4 pm)	7 °C (h.10 am); 6 °C (h.1 pm); 5 °C (h.4 pm)
Δ PET (2020–2050) at h.10; h.13; h.4 pm	2.2 °C (h.10 am); 2.5 °C (h.1 pm); 2.6 °C (h.4 pm)	2 °C (h.10 am); 2.5 °C (h.1 pm); 2.6 °C (h.4 pm)

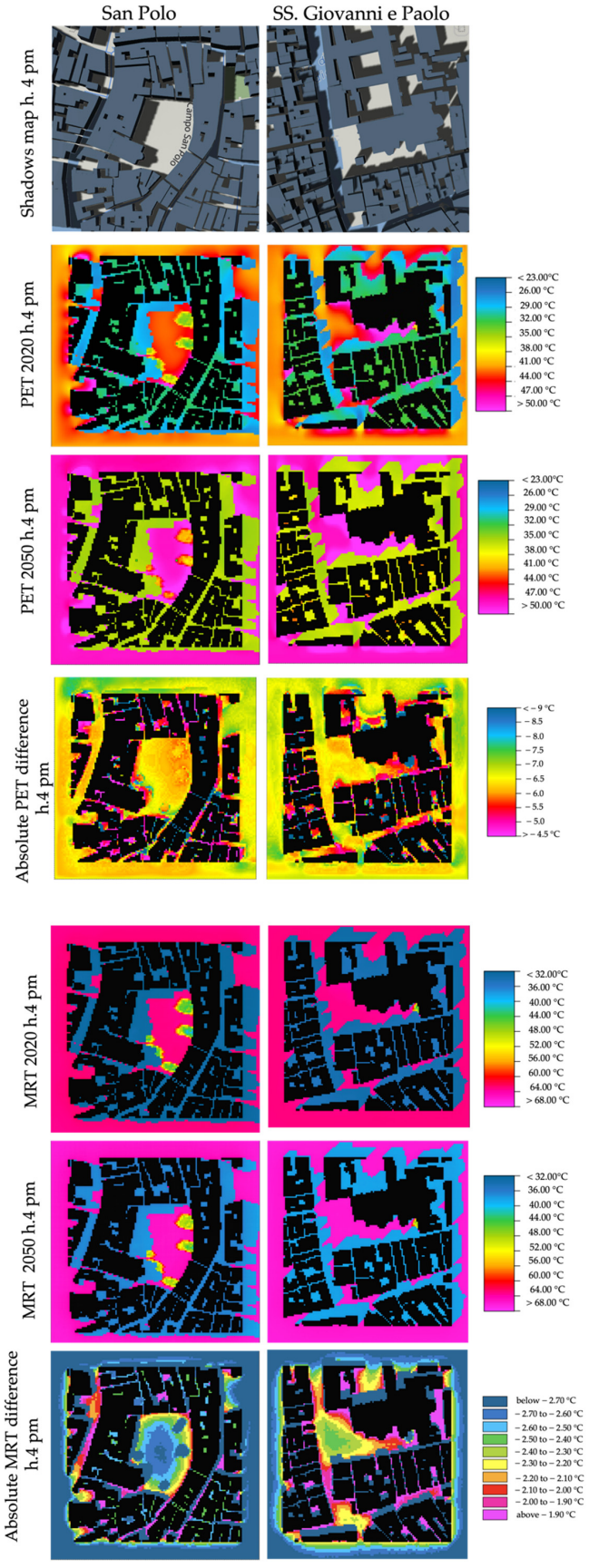

Figure 16. Comparative chart for PET values and MRT values, calculated at h. 4 pm in 2020 and 2050 projected scenario, for San Polo and SS. Giovanni e Paolo.

5. Discussion

Concerning the research questions, MRT and PET values, as well as considerations for building density and building height, are conducted for 2020 and 2050 projected scenarios.

5.1. MRT–PET in 2020

As reported in Table 4, orientation and the extension of the open and paved areas are the factors affecting microclimate.

In SS. Giovanni e Paolo, the shaded areas cast by the east side buildings and by the Church offer a greater reduction in the MRT of the *Campo*, especially during late afternoons and evenings (42% at h. 4 pm, almost 70% at h. 8 pm). In San Polo, shaded areas are less prolonged due to *Campo*'s wide width (70 m) (at hottest hours, the percentage of the shed area is negligible (16% at h.1 pm).

In SS. Giovanni e Paolo, higher compactness and a homogenous building height (mean height 11.57 m) decrease MRT by the canal.

In San Polo, the tight distance of the canals makes the infiltration of cool breezes difficult. MRT and PET values in 2020 are greatly affected by the shadow's distribution: in SS. Giovanni e Paolo, the shaded areas are more effective in lowering thermal discomfort while, in San Polo, the shaded areas are less extensive due to *Campo*'s large width, and thermal stress is more harmful.

5.2. MRT–PET in 2050

Similar results can be foreseen in the 2050 projection, but the urban form responds effectively to higher MRT and Pot values via high compactness.

In San Polo, where building heights are homogeneous (max height 26.6 m and mean height 12.62 m), the total built area compared to the total floor area of the fabric (FSI 2.29) is lower than SS. Giovanni e Paolo. Along with lower building coverage, the shaded areas are less effective in reducing thermal discomfort, as they are more successful in reducing Pot values near the eastern front. As in Table 4 and Figure 16, the orientation and *Campi* widths are the most effective elements in reducing thermal behaviour, as the presence of the canals is to be considered as a critical element due to heat storage, as well as given the scarce presence of still water.

MRT and PET values in 2050 are greatly affected by the shadow's distribution: in SS. Giovanni e Paolo, the shaded areas are more effective in lowering thermal discomfort, while, in San Polo, the shaded areas are less extensive due to *Campo*'s large width, and thermal stress is more harmful.

5.3. Thermal Resilience Potentialities

Generally, shaded areas allow for major thermal comfort both in 2020 and 2050. The highest thermal stress occurs in the middle of the *Campi*'s unshaded paved surfaces. At large, the nearby canals provide thermal storage due to a limited depth. Heat stress increases in the 2050 scenario.

It is worth highlighting that the influence of the impact of urban form on the microclimate processes of ventilation and shadow patterns mitigates thermal stress. Due to the high compactness of the urban fabric, *Campi* are the only open spaces that benefit from wind flows. This is clear when canals cross or are tangent to open spaces, such as in *Campo* SS. Giovanni e Paolo. Land cover and canal canyons facilitate cool breezes contributing to a lower PET.

The absolute difference in PET and MRT values (Figure 16) shows that San Polo is more resilient to climate change: the average absolute difference of PET is more homogeneous (5 °C at h.10 am to 6.5 °C at h. 4 pm).

In *Campo* SS. Giovanni e Paolo, the average absolute difference PET values vary from 7 °C at h.10 am to 5 °C at h. 4 pm.

In *Campo* San Polo, Δ PET is greater in 2020 than in 2050. Thermal discomfort in SS Giovanni e Paolo is less evident in 2020, while the 2050 scenario shows a noticeable Δ PET.

Generally, greenery scarceness is negligible in mitigating thermal stress in both *Campi*. In San Polo, the limited presence of trees can be observed in MRT value distribution, as in SS. Giovanni e Paolo, where the green mass is relegated inside a private cloister and does not influence thermal stress.

Similar considerations about thermal resilience potentialities can be partially extended to other dense urban archetypes. Among different parameters that affect outdoor thermal comfort, MRT and wind velocity have been proved to be influenced significantly by urban geometry, as assessed in previous studies on Dutch squares [41].

The analysis presented here suggests that the increased density of shadow areas can mitigate outdoor temperature values and reduce direct radiation on façades, reducing PET values, as already highlighted in previous studies, where urban form variables explain more than half of the variation in PET [53].

5.4. Limitation of the Study

Some limitations to the research should be noted since the results are based on a predictive study considering future conditions that may or may not occur.

First, a limited selection of building materials was used in the simulation. Three different building profiles for every building type in the selected *Campi* have been assessed as a homogenous building envelope's solution. Second, the number of Venice *Campi* case studies is small, if compared to many different *Campi* and their irregularity in size and shape. Third, the simulation period is 20 h during the hottest day. A 24/48 h computation should be preferred. Fourth, in the modelling, only public green was considered. The presence of green mass inside private courtyards has been neglected.

Fifth, as some studies have recently highlighted, ENVI-met underestimates MRT and consequently PET values, reporting lower values if compared to the values measured experimentally [54].

Lastly, the presence of the canals is simulated, but the cooling effect of water bodies due to evaporation is small on short timescales simulation; moreover, the influence of the Venice lagoon is neglected.

In addition, some real monitoring on-site is expected, as the UHI effect varies from simulation software's data to on-site temperature and relative humidity data.

6. Conclusions

To respond to the research aims, the thermal resilience of Venice's *Campi* today and in a future climate scenario was assessed. Appraisal of the strengthening resilience of built heritage relative to climate change-related heat waves in Venice was evaluated by comparing 2020 and 2050 scenarios in two typical Venetian open spaces, called *Campi:*

(i) Assessing today's thermal stress suggests that compact urban fabric decreases PET values due to the extensive project of shadows;
(ii) Assessing the thermal stresses in the projected 2050 climatic scenario shows how high density the factor resulting in mitigation is;
(iii) Venetian *Campi* were thought for functional and social purposes; this research study offers the perspective that they, in addition, grant some effective outdoor mitigations to face future heat waves. *Campi* may be an entity helping future climate change issues.

Author Contributions: Conceptualization, B.G. and E.N.; methodology, B.G. and D.M.; software, D.M.; validation, B.G., D.M. and E.N.; formal analysis, B.G. and D.M.; investigation, E.N., B.G. and D.M.; resources C.F. and M.M.; data curation, D.M. and B.G.; writing—original draft preparation, B.G.; writing—review and editing, E.N.; visualization, C.F.; supervision, E.N. All authors have read and agreed to the published version of the manuscript.

Funding: This research received no external funding.

Institutional Review Board Statement: Not applicable.

Informed Consent Statement: Not applicable.

Data Availability Statement: The authors wish to acknowledge simulation works by students and PhD candidates during Venice Workshop Venice 2050: Urban fabric and Climate Change held at the University of Parma, 7–18 December 2020.

Conflicts of Interest: The authors declare no conflict of interest.

References

1. IPCC 2013 Climate Change: The Physical Science Basis. In *Contribution of Working Group I to the Fifth Assessment Report of the Intergovernmental Panel on Climate Change*; Cambridge University Press: Cambridge, UK, 2013.
2. Kayser-Bril, N. Europe is Getting Warmer, and It's Not Looking Like it's Going to Cool Down Anytime Soon. 2018. Available online: https://www.europeandatajournalism.eu/eng/News/Data-news/Europe-is-getting-warmer-and-it-s-not-looking-like-it-s-going-to-cool-down-anytime-soon (accessed on 20 August 2021).
3. Hatvani-Kovacs, G.; Belusko, M.; Skinner, N.; Pockett, J.; Boland, J. Heat stress risk and Gertrud resilience in the urban environment. *Sustain. Cities Soc.* **2016**, *26*, 278–288. [CrossRef]
4. Santamouris, M. Recent progress on urban overheating and heat island research. Integrated assessment of the energy, environmental, vulnerability and health impact. Synergies with the global climate change. *Energy Build.* **2020**, *207*, 109482. [CrossRef]
5. Santamouris, M. Innovating to zero the building sector in Europe: Minimising the energy consumption, eradication of the energy poverty and mitigating the local climate change. *Sol. Energy* **2016**, *128*, 61–94. [CrossRef]
6. Europe One Degree Warmer. Available online: https://www.onedegreewarmer.eu/city/Venezia (accessed on 20 August 2021).
7. Carbognin, L.; Teatini, P.; Tomasin, A.; Tosi, L. Global change and relative sea level rise at Venice: What impact in term of flooding. *Clim. Dyn.* **2010**, *35*, 1039–1047. [CrossRef]
8. Braga, F.; Scarpa, G.M.; Brando, V.E.; Manfè, G.; Zaggia, L. COVID-19 lockdown measures reveal human impact on water transparency in the Venice Lagoon. *Sci. Total. Environ.* **2020**, *736*, 139612. [CrossRef] [PubMed]
9. Peron, F.; De Maria, M.; Spinazzè, F.; Mazzali, U. An analysis of the urban heat island of Venice mainland. *Sustain. Cities Soc.* **2015**, *19*, 300–309. [CrossRef]
10. Naboni, E.; Havinga, L.C. *Regenerative Design in Digital Practice. A Handbook for the Built Environment*; EURAC: Bolzano, Italy, 2019.
11. Adolphe, L. A Simplified Model of Urban Morphology: Application to an Analysis of the Environmental Performance of Cities. *Environ. Plan. B Plan. Des.* **2001**, *28*, 183–200. [CrossRef]
12. Sharifi, A.; Yamagata, Y. Principles and criteria for assessing urban energy resilience: A literature review. *Renew. Sustain. Energy Rev.* **2016**, *60*, 1654–1677. [CrossRef]
13. Natanian, J.; Aleksandrowicz, O.; Auer, T. A parametric approach to optimizing urban form, energy balance and environmental quality: The case of Mediterranean districts. *Appl. Energy* **2019**, *254*, 113637. [CrossRef]
14. Nik, V.M.; Perera, A.T.D.; Chen, D. Towards climate resilient urban energy systems: A review. *Natl. Sci. Rev.* **2021**, *8*, nwaa134. [CrossRef]
15. Abdollahzadeh, N.; Biloria, N. Outdoor thermal comfort: Analyzing the impact of urban configurations on the thermal performance of street canyons in the humid subtropical climate of Sydney. *Front. Arch. Res.* **2021**, *10*, 394–409. [CrossRef]
16. Ratti, C.; Baker, N.; Steemers, K. Energy consumption and urban texture. *Energy Build.* **2005**, *37*, 762–776. [CrossRef]
17. Cheng, V.; Steemers, K.; Montavon, M.; Compagnon, R. Urban Form, Density and Solar Potential. In Proceedings of the PLEA2006—23rd Conference Passiv, Low Energy Architecture, Geneva, Switzerland, 6–8 September 2006.
18. Zhang, J.; Heng, C.K.; Malone-Lee, L.C.; Hii, D.J.C.; Janssen, P.; Leung, K.S.; Tan, B.K. Evaluating environmental implications of density: A comparative case study on the relationship between density, urban block typology and sky exposure. *Autom. Constr.* **2012**, *22*, 90–101. [CrossRef]
19. Salvati, A.; Coch, H.; Morganti, M. Effects of urban compactness on the building energy performance in Mediterranean climate. *Energy Procedia* **2017**, *122*, 499–504. [CrossRef]
20. EU Project "Climate for Culture", Damage Risk Assessment, Economic Impact and Mitigation Strategies for Sustainable Preservation of Cultural Heritage in Times of Climate Change. Available online: https://www.climateforculture.eu/index.php?inhalt=home (accessed on 6 October 2021).
21. Matzarakis, A.; Amelung, B. Physiological Equivalent Temperature as Indicator for Impacts of Climate Change on Thermal Comfort of Humans. In *Seasonal Forecasts, Climatic Change and Human Health*; Springer: Amsterdam, The Netherlands, 2008; pp. 161–172.
22. Alberti, M.; Marzluff, J.M. Ecological resilience in urban ecosystems: Linking urban patterns to human and ecological functions. *Urban Ecosyst.* **2004**, *7*, 241–265. [CrossRef]
23. Doulos, L.; Santamouris, M.; Livada, I. Passive cooling of outdoor urban spaces. The role of materials. *Sol. Energy* **2004**, *77*, 231–249. [CrossRef]
24. Brown, R.D.; Vanos, J.; Kenny, N.; Lenzholzer, S. Designing urban parks that ameliorate the effects of climate change. *Landsc. Urban Plan.* **2015**, *138*, 118–131. [CrossRef]
25. Ratti, C.; Raydan, D.; Steemers, K. Building form and environmental performance: Archetypes, analysis and an arid climate. *Energy Build.* **2003**, *35*, 49–59. [CrossRef]

26. Noro, M.; Lazzarin, R. Urban heat island in Padua, Italy: Simulation analysis and mitigation strategies. *Urban Clim.* **2015**, *14*, 187–196. [CrossRef]
27. Naboni, E.; Natanian, J.; Brizzi, G.; Florio, P.; Chokhachian, A.; Galanos, T.; Rastogi, P. A digital workflow to quantify regenerative urban design in the context of a changing climate. *Renew. Sustain. Energy Rev.* **2019**, *113*, 109255. [CrossRef]
28. Santamouris, M. On the energy impact of urban heat island and global warming on buildings. *Energy Build.* **2014**, *82*, 100–113. [CrossRef]
29. Brown, G.Z.; DeKay, M. *Sun, Wind and Light. Architectural Design Strategies*, 2nd ed.; John Wiley & Sons: New York, NY, USA, 2001.
30. Givoni, B. *Urban. Design in Different Climates*; World Meteorological Organization: WMO/TD n.346. WTO: Geneva, Switzerland, 1989.
31. European Urban Charter II. In *Manifesto for a New Urbanity*; Council of Europe Publishing: Strasbourg, France, 2008.
32. Li, Y.; Schubert, S.; Kropp, J.P.; Rybski, D. On the influence of density and morphology on the Urban Heat Island intensity. *Nat. Commun.* **2020**, *11*, 1–9. [CrossRef] [PubMed]
33. Scarpa, T. *Venezia è un Pesce. Una Guida*; Feltrinelli: Milano, Italy, 2000.
34. Muratori, S. *Studi per un'Operante Storia Urbana di Venezi*; Istituto Poligrafico dello Stato: Roma, Italy, 1960; pp. 29–35.
35. Crowhurst Lennard, S.H. The Venetian Campo. In *Ideal setting for Social Life and Community*; Corte del Fontego: Venezia, Italy, 2012.
36. Berghauser Pont, M.; Haupt, P. *Space—Matrix: Space, Density and Urban Form*; Architecture Institute: Amsterdam, The Netherlands, 2010.
37. Erbani, F. *Non è Triste Venezia. Pietre, Acque, Persone. Reportage Narrativo da una Città che deve Ricominciare*; Manni Editore: San Cesario di Lecce, Italy, 2018.
38. Bruse, M. The Influences of Local Environmental Design on Microclimate—Development of a Prognostic Numerical Model ENVI-Met for the Simulation of Wind, Temperature, and Humidity Distribution in Urban Structures. Ph.D. Thesis, University of Bochum, Bochum, Germany, 1999.
39. Bruse, M.; Fleer, H. Simulating surface–plant–air interactions inside urban environments with a three dimensional numerical model. *Environ. Model. Softw.* **1998**, *13*, 373–384. [CrossRef]
40. Salata, F.; Golasi, I.; Vollaro, R.D.L.; Vollaro, A.D.L. Urban microclimate and outdoor thermal comfort. A proper procedure to fit ENVI-met simulation outputs to experimental data. *Sustain. Cities Soc.* **2016**, *26*, 318–343. [CrossRef]
41. Taleghani, M.; Kleerekoper, L.; Tenpierik, M.; van den Dobbelsteen, A. Outdoor thermal comfort within five different urban forms in the Netherlands. *Build. Environ.* **2015**, *83*, 65–78. [CrossRef]
42. Crank, P.J.; Sailor, D.J.; Ban-Weiss, G.; Taleghani, M. Evaluating the ENVI-met microscale model for suitability in analysis of targeted urban heat mitigation strategies. *Urban Clim.* **2018**, *26*, 188–197. [CrossRef]
43. Ambrosini, D.; Galli, G.; Mancini, B.; Nardi, I.; Sfarra, S. Evaluating mitigation effects of urban heat islands in a historical small center with the ENVI-Met climate model. *Sustainability* **2014**, *6*, 7013–7029. [CrossRef]
44. Ibrahim, Y.I.; Kershaw, T.; Shepherd, P. A methodology For Modelling Microclimate: A Ladybug-tools and ENVI-met Verification Study. In Proceedings of the 35th PLEA Conference Sustainable Architecture and Urban Design, a Coruña, Spain, 1–3 September 2020.
45. Perini, K.; Chokhachian, A.; Dong, S.; Auer, T. Modeling and simulating urban outdoor comfort: Coupling ENVI-Met and TRNSYS by grasshopper. *Energy Build.* **2017**, *152*, 373–384. [CrossRef]
46. Available online: https://energyplus-weather.s3.amazonaws.com/europe_wmo_region_6/ITA/ITA_Venezia-Tessera.161050_IGDG/ITA_Venezia-Tessera.161050_IGDG.zip (accessed on 20 August 2021).
47. Remund, J.; Müller, S.C.; Schilter, C.; Rihm, B. The Use of Meteonorm Weather Generator for Climate Change Studies. In Proceedings of the 10th EMS Annual Meeting, 10th European Conference on Applications of Meteorology (ECAM) Abstracts, Zürich, Switzerland, 13–17 September 2010.
48. IPCC. Special Report Summary for Policymakers. In *Emissions Scenarios*; IPCC: Geneva, Switzerland, 2000.
49. Available online: https://shadowmap.org (accessed on 15 July 2021).
50. Atlante della Laguna. Available online: http://www.atlantedellalaguna.it/?q=maps#tema-1-titolo (accessed on 20 August 2021).
51. Capedri, S.; Grandi, R.; Venturelli, G. Trachytes Used for Paving Roman Roads in the Po Plain: Characterization by Petrographic and Chemical Parameters and Provenance of Flagstones. *J. Archaeol. Sci.* **2003**, *30*, 491–509. [CrossRef]
52. Höppe, P. The physiological equivalent temperature–a universal index for the biometeorological assessment of the thermal environment. *Int. J. Biometeorol.* **1999**, *43*, 71–75. [CrossRef]
53. Galal, O.M.; Sailor, D.J.; Mahmoud, H. The impact of urban form on outdoor thermal comfort in hot arid environments during daylight hours, case study: New Aswan. *Build. Environ.* **2020**, *184*, 107222. [CrossRef]
54. Tsoka, S.; Tsikaloudaki, K.; Theodosiou, T. Analyzing the ENVI-met microclimate model's performance and assessing cool materials and urban vegetation applications—A review. *Sustain. Cities Soc.* **2018**, *43*, 55–76. [CrossRef]